Open Research Online

The Open University's repository of research publications
and other research outputs

Partial kindling induces neurogenesis, activates astrocytes and alters synaptic morphology in the dentate gyrus of freely moving adult rats

Journal Item

For guidance on citations see FAQs.

Version: [not recorded]

Link(s) to article on publisher's website:
http://dx.doi.org/doi:10.1016/j.neuroscience.2009.05.020

oro.open.ac.uk

Accepted Manuscript

PARTIAL KINDLING INDUCES NEUROGENESIS, ACTIVATES ASTROCYTES AND ALTERS SYNAPTIC MORPHOLOGY IN THE DENTATE GYRUS OF FREELY MOVING ADULT RATS

Igor V. Kraev, Oleg V. Godukhin, Ilya V. Patrushev, Heather A. Davies, Victor I. Popov, Michael G. Stewart
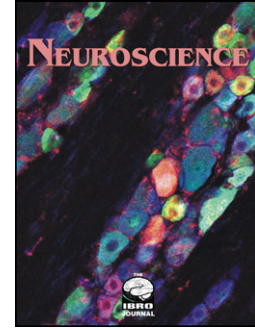
Please cite this article as: Kraev, I.V., Godukhin, O.V., Patrushev, I.V., Davies, H.A., Popov, V.I., Stewart, M.G., PARTIAL KINDLING INDUCES NEUROGENESIS, ACTIVATES ASTROCYTES AND ALTERS SYNAPTIC MORPHOLOGY IN THE DENTATE GYRUS OF FREELY MOVING ADULT RATS, *Neuroscience* (2009), doi: 10.1016/j.neuroscience.2009.05.020.

Section editor   **Prof Menahem Segal**

PARTIAL KINDLING INDUCES NEUROGENESIS, ACTIVATES ASTROCYTES AND ALTERS SYNAPTIC MORPHOLOGY IN THE DENTATE GYRUS OF FREELY MOVING ADULT RATS

Igor V. Kraev[1,2], Oleg V. Godukhin[3,4], Ilya V.Patrushev[2], Heather A. Davies[1], Victor I. Popov[1,2], and Michael G. Stewart[1].

[1] The Open University, Department of Life Sciences, Milton Keynes MK7 6AA, United Kingdom. (popvi@mail.ru and m.g.stewart@open.ac.uk); [2] Institute of Cell Biophysics, Russian Academy of Sciences, Pushchino 142290, Russia; [3] Institute of Theoretical and Experimental Biophysics, Russian Academy of Sciences, Pushchino 142290, Russia; [4] Pushchino State University, Pushchino, 142290, Russia

Correspondence to: Michael G. Stewart, Department of Life Sciences, Faculty of Sciences, The Open University, Walton Hall, Milton Keynes, MK7 6AA, UK. Telephone +44 1908-858192, Fax +44 1908-654167. E-mail address: m.g.stewart@open.ac.uk

Abbreviations: BrdU, 5-bromo-2-deoxyuridine; DCX, doublecortin; DG, dentate gyrus; GFAP, glial fibrillary acidic protein.

ABSTRACT

A partial kindling procedure was used to investigate the correlation between focal seizure development and changes in dendritic spine morphology, ongoing neurogenesis and reactive astrogliosis in the adult rat dentate gyrus (DG).

The processes of neurogenesis and astrogliosis were investigated using markers for doublecortin (DCX), BrdU and glial fibrillary acidic protein (GFAP). Our data demonstrate that mild focal seizures induce a complex series of cellular events in the DG one day after cessation of partial rapid kindling stimulation consisting (in comparison to control animals that were electrode implanted but unkindled), firstly, of an increase in the number of postmitotic BrdU labelled cells, and secondly, an increase in the number of DCX labelled cells, mainly in subgranular zone. Ultrastructural changes were examined using qualitative electron microscope analysis and 3-D reconstructions of both dendritic spines and postsynaptic densities. Typical features of kindling in comparison to control tissue included translocation of mitochondria to the base of the dendritic spine stalks; a migration of multivesicular bodies into mushroom dendritic spines, and most notably formation of "giant" spinules originating from the head of the spines of DG neurons. These morphological alterations arise at seizure stages 2-3 (focal seizures) in the absence of signs of the severe generalized seizures that are generally recognized as potentially harmful for neuronal cells.

We suggest that an increase in ongoing neurogenesis, reactive astrogliosis and dendritic spine reorganization in the DG are the crucial steps in the chain of events leading to the progressive development of seizure susceptibility in hippocampal circuits.

Key words: kindling, neurogenesis, astrocytes, synapse, spines, 3D reconstructions

Kindling is not only a model of epileptogenesis (in conditions where "seizures beget seizures") but can be considered as a model of a "pathological" form of neuroplasticity which is responsible for the development of cellular- molecular and network events producing the disordered firing of subpopulations of neurons (Goddard, 1967; Goddard et al., 1969; McEachern and Shaw, 1996; McIntyre et al., 2002; Racine, 1972; Sutula, 2004). In the conventional kindling paradigm, stimulations are delivered once or twice daily during 2 − 3 weeks, until the rats have experienced 3 consecutive grade 5 seizures (generalized seizures or fully kindled animals). In the partial kindling paradigm, the number of stimulations is much smaller, and the rats show only focal seizures but not the signs of generalized seizure response (Engel et al., 1978; Liu and Leung, 2003). This comparatively mild kindling stimulation is not accompanied by visible neuronal death (Tuunanen and Pitkanen, 2000) and can be used for precise analysis of specific morphological alterations underlying the induction mechanisms of focal epileptogenesis. In addition, recent investigations have indicated that the rapid protocol of kindling stimulation provides an opportunity to test, in a highly controlled manner, the effect of seizures alone with regard to neuronal injury and regeneration (Smith et al., 2005).

In spite of intensive studies, the mechanisms of kindling development remain unresolved. It is known that the dentate gyrus (DG) plays a crucial role in regulating excitability within the limbic system (Ratzliff et al., 2002) and is a control point for epileptogenesis in hippocampal circuits (Lothman et al., 1992). As proposed, the DG regulates or 'filters' the flow of paroxysmal activity in hippocampal circuits. However, the findings concerning morphological changes in the DG in relation to kindling development are somewhat contentious.

In fully kindled animals, in conditions where neuronal cell loss can be detected after generalized convulsions, and the relationship between cause and effect is uncertain, a variety

of permanent structural changes in the DG after kindling stimulations have been observed (Bengzon et al., 1997; Cavazos and Sutula, 1990; Lynch and Sutula, 2000, Smith et al., 2006). However, in contrast, other studies have claimed to show that amygdala kindling either does not reduce total neuronal number in the amygdala or hilus of DG after only a few seizures (Tuunanen and Pitkanen, 2000), or that there is an increase of only a small number of TUNEL positive cells (a marker of programmed cell death) after amygdala kindling-induced seizures (stage 3 of behavioural seizures) (Umeoka et al., 2000).

A causal relationship between ongoing adult neurogenesis and kindling epileptogenesis is also unresolved. Adult generated neurons in the DG become functionally integrated into the existing hippocampal circuit by forming synapses with mature neurons (Ide et al., 2008; Zhao and Overstreet-Wadiche, 2008). However, whether these changes contribute to or counteract epileptogenesis remains the subject of intensive investigations. Histological examination has demonstrated that severe repeated epileptic seizures cause overt neuronal cell death and increase the rate of neurogenesis in the limbic system (Bengzon et al., 1997; Mohapel et al., 2004; Park et al., 2006). These findings suggest that seizure-induced neurogenesis reflects an adaptive response to seizure-induced neuronal death rather than kindling development per se.

Recent studies using modern 3-dimensional electron microscopy reconstruction techniques indicate that dendritic spines can change their morphology and ultrastructure during long-lasting plastic modifications of synaptic activity (Popov et al., 2004; Matsuzaki et al., 2004; Leite et al., 2005; Ribak, Shapiro, 2007). These data raise the possibility that in mature synapses, entry of Ca^{2+} through activated NMDA receptor channels may be involved in remodelling of the postsynaptic membrane, which in turn may contribute to a change in synaptic efficacy during kindling epileptogenesis. Indeed, previous work using the conventional kindling paradigm and single-section analysis of electron microscope sections have demonstrated that hippocampal kindling induces increases in the mean area of post-

synaptic density of perforated synapses and increases in the number of axospinous synapses with segmented postsynaptic densities in the hippocampus (Geinisman et al., 1990; Geinisman et al., 1992). However, it is unclear whether these changes contribute to the mechanisms of neuroplasticity underlying specific morphological alterations related to kindling development or reflect an adaptive response to seizure-induced neuronal death.

In the present study, to analyse specific morphological alterations underlying the induction mechanisms of focal epileptogenesis, we used the partial rapid kindling procedure to correlate changes in structure of spines and synapses, and in adult neurogenesis and astrocyte activation, with alterations in EEG-after discharge (AD) duration in the DG. Quantitative electron microscope morphometric analysis and 3D reconstructions of both dendritic spines and postsynaptic densities (PSDs) in the ipsi- and contralateral (to the site of stimulation) DG were made on serial ultrathin sections. In addition, we investigated the process of neurogenesis using doublecortin (DCX), a marker of migrating progenitor neuronal cells (Brown et al., 2003; Francis et al. 1999; Gleeson et al., 1999), and another phenotypic marker (BrdU) for proliferating cells. Furthermore, reactive astrogliosis using as a marker a glial fibrillary acidic protein (GFAP) was also investigated in our experiments since astrocytes play a key role in the pathological and regenerative responses to various insults in the brain (Chen and Swanson, 2003; Hailer et al., 2001).

Experimental procedures

Animals and Surgery. Eight male Wistar rats weighing 300 – 350 g at the time of the surgery were used. All rats were treated in accordance to the guidelines approved by the European Ethics Committee (decree 86/609/CEE). Animals were anesthetized by intraperitoneal injection of sodium pentobarbital (60 mg/kg) and mounted in a stereotaxic frame. A tripolar nichrome electrode was implanted into the right DG according to the following coordinates: 3.0 mm posterior to bregma, 3.7 mm right of midline, and 3.8 mm ventral to the skull

(Pellegrino et al., 1979). The bipolar stimulation / unipolar recording electrode unit to provide AD recording from the stimulation focus was fixed to the skull with dentate acrylic cement. A screw electrode was placed in the right frontal skull as a reference.

Rapid partial kindling procedures. Experiments commenced one week after surgery. In the kindled group (n = 4) the rats were electrically stimulated according to the serial day rapid kindling model (De Smedt et al., 2005). Four rats control rats received matched handling and electrode implantation, but no stimulation. Kindled rats received 12 stimulations daily, on consecutive days (for three days). Each stimulation consisted of a 9 s train of 0.1 ms square wave pulses at an intensity (300-400 A) of the threshold that evoked AD duration of about $10 - 20$ s. The stimulation frequency was set at 20 Hz. ADs were identified where the EEG responses were more then 3-4 times higher in comparison to the background EEG. Consecutive stimulations were spaced 30 min apart, and the kindling response was evaluated on the EEG (AD pattern and AD duration) and in accordance to behavioural seizures. The after discharge (AD) pattern and AD duration were analyzed off-line using software developed in house. The severity of the behavioural seizures were scored following visual inspection in accordance to the modified scale of Racine (1972): stage 1, wet dog shakes; stage 2, wet dog shakes + chewing; stage 3, wet dog shakes + chewing + forelimb clonus; stage 4, forelimb clonus with rearing; stage 5, clonus with rearing and falling on the back. The partial kindled group for light and electron microscopy included only those rats that did not show behavioural signs of stages 4-5 generalized seizure responses during the stimulation procedure.

BrdU-injections. One hour before the start of kindling stimulations, each of 8 rats (as described above) received daily, a BrdU (50 μg/g, i.p.) injection on the 1st, 2nd and 3rd stimulation days. BrdU (Abcam, UK) was dissolved in 0.9% saline. One day after the last BrdU injection, animal were sacrificed and prepared for light and electron microscopy.

Tissue preparation. The rats were injected with an overdose of ketamine and perfused

transcardially with 30 ml physiological saline, followed by 300 ml of 0.5% glutaraldehyde and 4% paraformaldehyde in 0.1 M phosphate buffer (PB), pH 7.4. The brains were stored in the fixative overnight. 50 μm coronal sections were cut on vibrating microtome (Leica, Germany).

Antibodies. DCX and GFAP immunohistochemistry. All antibodies were diluted in 0.1 M phosphate buffer (pH 7.4) containing 0.05% Triton X-100 and 2% fish gelatin (Sigma) (incubation buffer). The primary antibodies used in this study were: monoclonal rat anti-BrdU (cat. № ab6326-250, Abcam, UK), 1:100; polyclonal rabbit anti-DCX (cat. № ab18723, Abcam, UK), 1:200; and monoclonal mouse anti-GFAP (cat. № ab4648-100, Abcam, UK), 1:500. For immunohistochemistry with the peroxidase technique, biotinylated donkey anti-rat IgG (cat. № 712-065-150, Jackson, USA) (1:200) was used as secondary antibody and detected with avidinbiotin-peroxidase complex (ABC, Vectastain Elite, Vector Laboratories, UK) (9 μl/ml).

BrdU immunohistochemistry. After quenching endogenous tissue peroxidases with 1% sodium borohydride in PB for 30 minutes the sections were incubated in 2 M HCl for 30 min at 37°C and washed in borate for 5 minutes. The 50 μm sections were blocked in incubation buffer for 2 hours, followed by incubation in primary antibody in incubation buffer overnight at 4°C. After rinses in PB, the sections were incubated in the secondary antibody in incubation buffer for 4 hours at room temperature. After another set of rinses, ABC Elite reagent (Vector Laboratories, UK) was applied for 1 hour. As substrate for the peroxidase reaction, diaminobenzedine (DAB, Sigma, USA) was applied for 5 minutes at a concentration of 0.22 mg/ml in Tris buffer (pH 7.4) with 0.01% hydrogen peroxide. Sections were thoroughly washed, mounted, air dried, dehydrated and coverslipped. To control for non-specific labelling, adjacent sections were incubated without primary or secondary antibody; no labelling was detected following this procedure.

Quantification. Sampling of BrdU-positive cells was done exhaustively throughout the dentate gyrus in dorsal left and right hippocampi. Cells were categorized according to their localization in the dentate gyrus of both sides.

Hippocampal volume. In order to determine cell number accurately it is necessary to know the volume of the tissue within which the cells are present. Measurements of the volume of the dorsal hippocampus were made using the Cavalieri principle (as described in Popov et al., 2004). Serial coronal sections (50 μm thick) were collected and the total number of sections and their order were noted. The dorsal portion of the hippocampus occupied ~55 serial 50-μm sections. From the complete rostrocaudal set of sections through the dorsal anterior hippocampus in each animal, every third section in the series was mounted in section order onto glass slides, air dried and subsequently stained with a solution of 0.1% toluidine blue in 0.1 M phosphate buffer (pH 7.4) for 2 min. Sections were then washed, dehydrated in an ascending series of alcohols, passed through xylene and finally embedded in DPX. Sections were subsequently viewed and analysed at low magnification in a Nikon E800 digital photomicroscope. Images were aligned as JPEG images. Alignments were made with full-field images. Direct measurement of volume of dorsal hippocampus (of both right and left hemispheres) was made via the Trace program (http://synapse-web.org/tools/index.stm). Data are presented as mean ± SD. Statistical comparisons on volume data between groups of animals were performed using one-way ANOVA.

Relative volume of astrocytes. Using "Trace" (Drs. J.Fiala and K.Harris (http://synapse-web.org/tools/index.stm) we determined the relative volume of astrocytes from the hilus for all animals. The volume of astrocytes in left hippocampus of control rats was taken as 100%. After immunostaining with GFAP a 50 ⌈m thick slice contains an entire two-dimensional projection of many astrocytes including cell bodies and their cell processes. The image of each astrocyte was contoured and volume determined via "Trace" (see: Fig. 5), allowing a comparison of astrocytes size in each hemisphere. This program allows determination of the

volume of each contoured structure when section thickness is known and we used 50 ⌈m sections for immunolabelling. These sections contain mostly all of the astrocytes and their cell processes. The final microscopic image of each astrocyte thus represents a two-dimensional projection. The trace automatically gives the volume of each contoured cell. Such an approach is similar to densitometry of two-dimensional cell profiles. A comparison of the volume figures obtained of the astrocytes allows an estimation of the relative volume of the cells at the different functional state of brain tissue. Thus, in effect we used the Trace program as a densitometer. For the right hippocampi, analysis of astrocytes was made on images where scars were absent and 100 astrocytes per animal for left and right hippocampus were used. Data are presented as mean ± SD.

Electron microscopy. Briefly six 3-month old animals (3 trained and 3 untrained) animals were anaesthetised with sodium pentobarbital (100 mg/kg, i.p.) and transcardially perfused with 0.5% glutaraldehyde and 2.0 % paraformaldehyde. Coronal vibratome sections (50⌈m in thick) were taken in the hippocampal region and the slices fixed further by immersion in 0.1 M Na-cacodylate buffer (pH 7.2–7.3) containing 2.5% glutaraldehyde for 1–2 h at room temperature, followed by three washes in 0.1 M Na-cacodylate buffer. The tissue was post-fixed with 1% osmium tetroxide and 0.01% potassium dichromate in 0.1 M Na-cacodylate buffer for 1–1.5 h at room temperature. Subsequent processing for electron microscopy was exactly as described previously (Popov et al. 2004; Stewart et al., 2005). Blocks were trimmed as described by Popov et al. (2004) to include both supragranular and subgranular (hilar portion) layers. Serial sections were cut with a Diatome diamond knife and allowed to form a ribbon in the knife bath of 800-1000 serial sections. These were broken into series of 15-20 sections, collected on pioloform-coated slot grids and counterstained with saturated ethanolic uranyl acetate followed by Reynolds lead citrate. The series were examined with a JEOL 1010 electron microscope and photographed at 6,000-10,000x magnification. Cross-sectioned myelinated axons, dendrites, and mitochondria spanning all sections provided a

fiduciary reference for initial alignment of serial sections. Section thickness was determined using the approach of Fiala and Harris (http://synapse-web.org/tools/index.stm). For serial electron microscopy we have studied synapses in the middle molecular layer of dentate gyrus.

Digital reconstructive analysis. Digitally scanned EM negatives with a resolution of 900 dpi were aligned as JPEG images (software available from Fiala and Harris (2001): http://synapses.bu.edu). Alignments were made with full-field images. Contours of individual cells and their elements were traced digitally and computed.

Statistical analysis. Excel software was used to organize the data from the immunocytochemistry studies. Statistica (StatSoft, Tulsa, OK, USA) was used to obtain means and SDs to perform statistical analyses, and the Kolmogorov-Smirnov and Shapiro-Wilk normality tests to compare distributions (criterion $P < 0.05$). ANOVAs followed by Bonferroni's or Tukey's unequal N honest significant differences tests were performed with the OriginPro 7.5. All data are presented as a mean $\pm$ SD.

Results

Seizure characteristics during partial rapid kindling stimulation. Fig.1 A demonstrates the after discharge (AD) patterns after 3 and 36 kindling stimulations. These patterns include three components of the AD. A primary component represents the groups of EEG-spike bursts (200 – 500 ms duration) with about 500 ms interburst interval (clonic ictal - like activity). A secondary component represents the continuous single EEG-spikes (tonic ictal - like activity). A tertiary component represents the regular single spike bursts with a 500 ms interburst interval (interictal - like activity). After the first three stimulations, a total duration of these AD components $(1 + 2 + 3)$ was 15 – 25 s (Fig. 1B). However, after 36 stimulations, the total AD duration has increased to 80 – 100 s. During the 36 stimulations, the animals

displayed mainly focal seizures (grade 1 – 3) (Fig. 1B).

BrdU-labelling. Fig. 2 illustrates the organization of a scar in the right hippocampus. We did not observe any significant differences in BrdU-labelling of scars between control and after kindling. BrdU-labelled cells occupy relatively large areas which are contoured by the black dotted line in Fig. 2A and Fig. 2B. Fig. 2 shows three types of BrdU-labelled cells: astrocytes (black arrows); astrocytes or immature granule cells (red arrows), and endothelial cells (blue arrows) which form blood vessels during angiogenesis at least during 10 days after implantation of electrodes (see: Methods). Fig. 2B,D show that BrdU-labelled cells were localized around the scar. Fig. 2D,E show BrdU-labelled cells in dentate gyrus including subgranular zone, supragranular layer, and molecular layer. Quantification of BrdU-labelled cells in the whole dentate gyrus (Fig. 3) shows that kindling stimulates significantly an increase in BrdU-labelling in the right hippocampus. This is clearly not due simply to the damage per se resulting from electrode implantation since the increase is absent not only in the contralateral hemisphere of kindled rats, but also the right hemisphere of control animals (implanted but non-kindled).

DCX- and GFAP-labelling. Fig. 4 shows DCX (Fig. 4A-B) and GFAP-labelling (Fig. 4C-F) in rats after partial kindling in the right hippocampus. Fig. 4A-B shows DCX-labelling, mainly of the subgranular zone (SBZ) of dentate gyrus. Visual analysis shows clearly that the SBZ of the dentate gyrus in right hippocampus contains comparatively more intensive DCX-labelling (Fig. 4B) in contrast to left hippocampus (Fig. 4A) where electrodes were absent. GFAP-labelling for left (non electrode) and right hippocampi (after kindling) is shown in Fig. 4C and Fig. 4D.

Quantification of GFAP-immunostaining for astrocytic volume is shown in Fig. 5. There is a significant difference between astrocytic volume in the right and left DG of control unstimulated rats, presumably due to the presence of the electrode in the right DG of the

unstimulated control rats. Surprisingly after kindling this difference disappears, due to an increase in astrocytic volume in the left unstimulated hemisphere. For comparison we show astrocyte images for left hippocampus (non electrode) of control (Fig. 4E) in comparison with right hippocampus after kindling (Fig. 4F).

Hippocampal volume was not significantly different between hemispheres or between control and kindled rats: for control the hippocampal volumes were 44.2 ± 0.8 (left hemisphere) vs 48.3 ± 5.8 mm^3 (right) (P=0.28460); and after kindling: 45.3 ± 4.9 (left) vs. 46.0 ± 5.0 mm^3 (P= 0.87086) (right).

Figure 6 shows DCX-labelling of granule cells localized in SGZ in agreement with that previously described by Ribak et al. (2004) and it corresponds to the distribution of newborn neurons in this brain region using other markers for newly generated neurons (Ribak et al 2004). No labelling of CA1-CA3 pyramidal neurons, or interneurons, was found in any hippocampal areas. The relatively intensive DCX-labelling of SGZ was apparent in both control and after kindling without significant differences. SGZ was discontinuous because DCX-labelled granule cells formed clusters (Seri et al., 2004; Ribak and Shapiro 2007) at low magnification (Fig. 6a). DCX-positive cells were mainly found in the SGZ at the hilar border. These cells appeared as cells with three processes: (1) Apical dendrite; (2) Basilar dendrite; and (3) Short mossy fibre with varicosities (Fig. 6 b-e). Short processes remained in the SGZ as described for recurrent basal dendrites (Ribak et al., 2004; Yan et al., 2001) (Fig. 6c-e). Most of these immunolabelled cells had apical dendrites, and many of them had bifurcating dendritic branches. Clusters of DBX-labelled neurons consisted of 4-6 neighbouring cells.

Electron microscopy. Qualitative comparison between kindled hippocampus and control tissue.

We did not observe any differences in the general appearance of control, and kindled

hippocampal tissue, compared to that which we have described in previous studies in normal hippocampal tissue. (Popov et al., 2004, 2005, 2008; Popov and Stewart, 2009). However, a more detailed examination of the tissue showed prominent ultrastructural changes after kindling in the right hippocampus. Fig. 7A-H shows 8 consecutive serial images of a dendrite with a thin dendritic spine. After kindling the mitochondrion moves to the base of the spine forming a tight contact (Fig. 7I-J); spine apparatus and cisterns of smooth endoplasmic reticulum were absent. Three-dimensional reconstruction of the relationship between the dendritic spine and mitochondrion is shown in Fig. 8 i-k. Another prominent feature of partial kindling is the growth of very long spinules (Fig. 8-9). Spinules with their double-walled membranes were readily distinguished from endosomal compartments, which have only a single coated or smooth plasma membrane (Fig. 9). Spinules originated from the heads of thin spines and penetrated neighbouring axonal varicosities including presynaptic boutons contacting with the spine (Fig. 8A-E). Five consecutive images show spinules originating from thin dendritic spine within presynaptic bouton (Fig. 8A-E). The three-dimensional structure of this spinule is shown in Fig. 8F-G. The length of the spinule is noticeably greater than that of the dendritic spine (Fig. 8G). Spinules occurred on all types of dendritic spines: all mushroom spines contained spinules whilst for thin spines only a fifth of the spines had a spinule. The shape of the spinules ranged from double-membrane pits to longer vermiform double-membrane structures. The relatively constricted base gave the impression that the invaginated structure was about to "engulf" or "pinch off" the evaginating structure. Occasionally, free double-walled structures were found in axons (Fig. 8E), in support of the hypothesis that spinules are undergoing trans-endocytosis (Popov et al., 2008; Sorra et al., 1998; Spacek and Harris, 2004). Three-dimensional reconstructions revealed that smooth endoplasmic reticulum (SER) similar to that described by Cooney et al. (2002) after kindling forms a network of thin tubules that occasionally widen into larger cisternae (Fig. 9). The tubules and cisternae generally were flattened, with an undulating

membrane. All lumens of the SER were electron lucent. SER was also continuous with the outer membrane of some mitochondria as described previously by Spacek and Lieberman (1980) and Popov et al. (2005). SER was located in the dendroplasm and extended into mushroom dendritic spines with perforated postsynaptic densities (PSDs) forming spine apparatus (Fig. 9). The spine apparatus is a prominent specialization of the SER found in mushroom spines. All large mushroom spines with perforated PSD contained spine apparatus and SER cisterns (Fig. 9). In addition to the spine apparatus many large mushroom spines contained multi-vesicular bodies (MVBs) in the vicinity of PSDs (Fig. 9D-F). Mitochondria occurred in the central part of the dendrite shaft, surrounded by the SER network (Fig. 8I-K).

Kindling stimulated formation of multi-synaptic boutons. The proportion of multi-synaptic boutons was increased by 24% in contrast to the right hippocampus without kindling.

Discussion

Our data have demonstrated that mild focal seizures induce a complex series of cellular events in the stimulated compared with both the contralateral (unstimulated) DG, and that of the right hemisphere of implanted but unkindled rats, 1 day after cessation of partial rapid kindling stimulation. Qualitative changes in ultrastructure were also examined, outside of the scar region of both kindled and control animals. The main events noted are:

1. an increase in the number of postmitotic BrdU labelled cells,

2. an increase in the number of DCX labelled cells mainly in subgranular zone,

3. translocation of mitochondria to the base of dendritic spine stalk of the neurons,

4. migration of multivesicular bodies into mushroom dendritic spines and

5. formation of "giant" spinules originating from spine head of the DG neurons.

There were no hippocampal volume changes following kindling but our data on

measurements of astrocytic volume (with an increase in the left hemisphere) show that the unstimulated contralateral hemisphere is affected when kindling occurs in the right hemisphere, indicating cross talk between hemispheres, though exactly how is unclear and will be the subject of a follow up investigation.

The alterations in the kindled hemisphere arise at the stage 2-3 (focal seizures) without the signs of severe generalized seizures that are potentially harmful for neuronal cells. Thus, with the initiation of kindling, repeated episodes of neuronal synchronization have the capacity to induce a complex series of cellular-molecular events leading to complicated structural alterations, such as neurogenesis, astrocyte activation and synaptic remodelling. Our data demonstrate that partial rapid kindling induces an increase in the number of DCX labelled cells. These cells were localized only in the subgranular zone at the hilar border (Figs. 4A-B, 7) and formed clusters consisting of 4-6 immature neurons, supporting findings from previous studies (Carnevale et al., 1997; Lauer et al., 2003; Ribak and Shapiro, 2007; Ribak et al., 2004; Shapiro et al., 2007, 2008). The seizure activity produced in this model of epileptogenesis induces neurogenesis in the granule cell layer of the DG without any appreciable induction of neuronal death in mice (Smith et al., 2006). The DG circuit restructuring is associated in all likelihood, specifically with kindling development but not with the stress response since, in contrast to our data, many stress-associated stimuli are capable of inducing neurogenesis in adult mammalian brain accompanying reductions of granule cell production and spine density (Bennur et al., 2007; Doetsch and Hen, 2005; Liu et al., 1998). Axons of adult-born granule cells can establish synapses with hilar interneurons, mossy cells, CA3 pyramidal cells, and release glutamate as their main neurotransmitter (Toni et al., 2008). These new granule cells in the adult DG can be incorporated into seizure-activated circuitry (Smith et al., 2006) and influence seizure development. When using the conventional kindling procedure, the increased proliferation of granule neurons was observed only during the later phases of kindling-induced

epileptogenesis (Scott et al., 1998). These authors indicated that in the early phases, when focal seizures were present, there was no evidence of a change in the rate of hippocampal neurogenesis. During the later phases of kindling, however, when secondary generalization was well established and motor seizures were present, neurogenesis was enhanced by 75 – 140 %.

Our results demonstrated that partial rapid kindling induces a notable increase in the number of postmitotic BrdU labelled cells. These cells were observed in the electrode scar zone mainly in subgranular and molecular layers of DG (Fig. 2E). In all likelihood, many BrdU labelled cells represent astrocytes because the same DG regions include a subset of GFAP expressing cells. Our findings are consistent with the observations of Khurgel and Ivy (1996) who have demonstrated that kindling-induced seizures result in a prominent hypertrophy and proliferation of astrocytes that are accompanied by a reorganization of astrocytic cytoskeleton. It is important to stress that these changes in astrocytes have been observed in the absence of overt neuronal degeneration. The changes in the morphology of astrocytes are seizure-intensity dependent, occur early in the kindling process, and persist for weeks following the last seizure.

In addition, our qualitative electron microscopic findings show that partial rapid kindling stimulates a translocation of mitochondria into the base of the dendritic spine stalk (Fig. 7-8). Such a translocation may be linked with calcium regulation within dendritic spine after electrical kindling stimulation and dendritic spines are also considered as calcium compartments (Segal, 2006). It is interesting to note that the dendritic spine with mitochondria at the base of dendritic spine stalk did not contain smooth ER. Cisterns of smooth ER and mitochondria represent two calcium compartments which are interconnected (Popov et al., 2005).

A prominent feature of dendritic spines after partial rapid kindling stimulation is the formation of "giant" spinules originating from the spine head (Fig. 8-9). Spinules between

mushroom spine heads and their presynaptic boutons usually occurred near the perforation or at the edge of the postsynaptic densities. The number of postsynaptic perforations and spinules on mushroom spines are known to increase after repeated frequency facilitation in the hippocampus (Applegate and Landfield, 1988), during intense stimulation of the frog forebrain with potassium chloride, and after tetanic or theta burst stimulation that induces long-term potentiation (LTP) (Schuster et al., 1990; Toni et al., 1999). Such perforations are thought to mark especially active synapses (Greenough et al., 1978; Edwards, 1995; Geinisman et al., 1995; Jones and Harris, 1995). According to Spacek and Harris (2004) cell adhesion molecules span the synaptic junction with links the underlying actin cytoskeleton. Recent evidence shows that the influx of calcium during repeated activation might cause the underlying actin cytoskeleton to "contract" (Matus et al., 2000), which might cause perforation and segmentation of the postsynaptic density. The cell adhesion molecules disassemble during LTP, which may weaken the links and allow perforations to form (Murase et al., 2002; Tang et al., 1998).

Our results also show that partial rapid kindling induces a translocation of multivesicular bodies to the mushroom dendritic spines (Fig. 9). It is possible that these bodies participate in the endocytotic process, translocating proteins and lipids to multiple cell sites including the cell surface, Golgi complex and lysosomes (Cooney et al., 2002; Kennedy and Ehlers 2006; Murk et al., 2003). It is interesting to note that partial rapid kindling stimulates an appearance of multisynaptic boutons but at present, their functional role in the neurons is still unknown (Popov and Stewart, 2009).

A key issue is the significance of the morphological changes obtained in our study with respect to development of kindling-induced seizures. Kindling is a form of neuronal plasticity produced by repeated low intensities electrical or chemical stimulations that leads to the progressive development of a permanent increase of seizure susceptibility. Partial rapid kindling paradigm allows investigation of the morpho-functional correlates of

mechanisms of neuroplasticity underlying an induction of focal epileptogenesis. The DG displays a rich structural and functional plasticity that can exert a regulatory role in the induction, maintenance or propagation of seizures. It is proposed that, depending on the circumstances, the DG can retard or reinforce seizure development. Our light and electron microscopic findings suggest that an increase in ongoing neurogenesis, reactive astrogliosis and dendritic spine reorganization in the DG are the important steps in the chain of events leading to the progressive development of seizure susceptibility in hippocampal circuits.

References

Applegate MD, Landfield PW (1988) Synaptic vesicle redistribution during hippocampal frequency potentiation and depression in young and aged rats. J Neurosci 8:1096–1111.

Bengzon J, Kokaia Z, Elmer E, Nanobashvili A, Kokaia M, Lindvall O (1997) Apoptosis and proliferation of dentate gyrus neurons after single and intermittent limbic seizures. Proc Natl Acad Sci USA 94:10432–10437.

Bennur S, Shankaranarayana Rao BS, Pawlak R, Strickland S, McEwen BS, Chattarji S (2007) Stress-induced spine loss in the medial amygdale is mediated by tissue-plasminogen activator. Neuroscience 144:8–16.

Brown JP, Couillard-Despres S, Cooper-Kuhn CM, Winkler J, Aigner L and Kuhn HG (2003) Transient expression of doublecortin during adult neurogenesis. J Comp Neurol 467:1–10.

Carnevale NT, Tsai KY, Claiborne BJ, Brown TH (1997) Comparative electrotonic analysis of three classes of rat hippocampal neurons. J Neurophysiol 78:703–720.

Cavazos JE, Sutula TP (1990) Progressive neuronal loss induced by kindling: a possible mechanism for mossy fiber synaptic reorganization and hippocampal sclerosis. Brain Res 527:1–6.

Chen Y, Swanson RA (2003) Astrocytes and brain injury. J Cereb Blood Flow Metab 23:137–149.

Cooney JR, Hurlburt JL, Selig DK, Harris KM, Fiala JC (2002) Endosomal compartments serve multiple hippocampal dendritic spines from a widespread rather than a local store of recycling membrane. J Neurosci 22:2215–2224.

Doetch F, Hen R (2005) Young and excitable: the function of new neurons in the adult mammalian brain. Cur Opin in Neurobiol 15:121–128.

De Smedt T, Vonck K, Raedt R, Deurwaerdere S, Claeys P, Legros B, Wyckhuys T, Wadman W, Boon P (2005) Rapid kindling in preclinical anti-epileptic drug development: the effect of levetiracetam. Epilepsy Res 67:109–116.

Edwards FA (1995) Anatomy and electrophysiology of fast central synapses lead to a structural model for long-term potentiation. Physiol Rev 75:759–787.

Engel JJ, Wolfson L, Brown L (1978) Anatomical correlates of electrical and behavioral events related to amygdaloid kindling. Ann Neurol 3:538–544.

Francis F, Koulakoff A, Boucher D, Chafey P, Schaar B, Vinet MC, Friocourt G, McDonnell N, Reiner O, Kahn A, McConnell SK, Berwald-Netter Y, Denoulet P, Chelly J (1999) Doublecortin is a developmentally regulated, microtubule-associated protein expressed in migrating and differentiating neurons. Neuron 23:247–256.

Geinisman Y, Morrell F, DeToledo-Morrell L (1990) Increase in the relative proportion of perforated axospinous synapses following hippocampal kindling is specific for the synaptic field of stimulated axons. Brain Res 507:325–331.

Geinisman Y, Morrell F, DeToledo-Morrell L (1992) Increase in the number of axospinous synapses with segmented postsynaptic densities following hippocampal kindling. Brain Res 569:341–357.

Gleeson JG, Lin PT, Flanagan LA, Walsh CA (1999) Doublecortin is a microtubule-associated protein and is expressed widely by migrating neurons. Neuron 23:257–271.

Greenough WT, West RW, DeVoogd TJ (1978) Subsynaptic plate perforations: changes with age and experience in the rat. Science 202:1096–1098.

Goddard GV (1967) Development of epileptic seizures through brain stimulation at low intensity. Nature 214:1020–1021.

Goddard GV, McIntyre DC, Leech CK (1969) A permanent change in brain function resulting from daily electrical stimulation. Exp Neurol 25:295–330.

Hailer NP, Wirjatijasa F, Roser N, Hischebeth GT, Korf HW, Dehghani F (2001) Astrocytic factors protect neuronal integrity and reduce microglial activation in an in vitro model of N-methyl-D-aspartate-induced excitotoxic injury in organotypic hippocampal slice cultures. Eur J Neurosci 14:315–326.

Ide Y, Fujiyama F, Okamoto-Furuta K, Tamamaki N, Kaneko T and Hisatsune T (2008) Rapid integration of young newborn dentate gyrus granule cells in the adult hippocampal circuitry. Eur J Neurosci 28:2381–2392.

Jones DG, Harris RJ (1995) An analysis of contemporary morphological concepts of synaptic remodelling in the CNS: perforated synapses revisited. Rev Neurosci 6:177–219.

Kennedy MJ, Ehlers MD (2006) Organelles and trafficking machinery for postsynaptic

plasticity. Annu Rev Neurosci 29:325–362.

Khurgel M, Ivy GO (1996) Astrocytes in kindling: relevance to epileptogenesis. Epilepsy Res 26:163–175.

Lauer M, Beckmann H, Senitz D (2003) Increased frequency of dentate granule cells with basal dendrites in the hippocampal formation of schizophrenics. Psychiatry Res 122:89–97.

Leite JP, Neder L, Arisi GM, Carlotti CG Jr, Assirati JA, Moreira JE (2005) Plasticity, synaptic strength, and epilepsy: what can we learn from ultrastructural data? Epilepsia 46 (Suppl 5):134–141.

Liu J, Solway K, Messing RO, Sharp FR (1998) Increased neurogenesis in the dentate gyrus after transient global ischemia in gerbils. J Neurosci 18:7768–7778.

Liu X, Leung LS (2003) Partial hippocampal kindling increases GABA$_B$ receptor-mediated postsynaptic currents in CA1 pyramidal cells. Epilepsy Res 57:33–47.

Lothman EW, Stringer JL and Bertran EH (1992) The dentate gyrus as a control point for seizures in the hippocampus and beyond. The Dentate Gyrus and Its Role in Seizures (Epilepsy Res. Suppl. 7, 301-313), Ed. by Ribak et al., Elsev. Science Publishers.

Lynch M, Sutula T (2000) Recurrent excitatory connectivity in the dentate gyrus of kindled and kainic acid-treated rats. J Neurophysiol 83:693–704.

Matsuzaki M, Honkura N, Ellis-Davies GCR, Kasai H (2004) Structural basis of long-term potentiation in single dendritic spines. Nature 429:761–776.

Matus A, Brinkhaus H, Wagner U (2000) Actin dynamics in dendritic spines: a form of regulated plasticity at excitatory synapses. Hippocampus 10:555–560.

McEachern JC, Shaw CA (1996) An alternative to the LTP orthodoxy: a plasticity-pathology continuum model. Brain Res Rev 22:51–92.

McIntyre DC, Poulter MO, Gilby K (2002) Kindling: some old and some new. Epilepsy Res 50:79–92.

Mohapel P, Ekdahe CT, Lindvall O (2004) Status epilepticus severity influences the long-term outcome of neurogenesis in the adult dentate gyrus. Neurobiol Dis 15:196–205.

Murase S, Mosser E, Schuman EM (2002) Depolarization drives beta-Catenin into neuronal spines promoting changes in synaptic structure and function. Neuron 35:91–105.

Murk JL, Humbel BM, Ziese U, Griffith JM, Posthuma G, Slot JW, Koster AJ, Verkleij AJ, Geuze HJ, Kleijmeer MJ (2003) Endosomal compartmentalization in three dimensions: implications for membrane fusion. Proc. Natl. Acad. Sci. USA 100:13332–13337.

Park JH, Cho H, Kim H, Kim K (2006) Repeated brief epileptic seizures by pentylenetetrazole cause neurodegeneration and promote neurogenesis in discrete brain regions of freely moving adult rats. Neuroscience 140:673–684.

Pellegrino LJ, Pellegrino AS, Cushman AJ (1979) A stereotaxic atlas of the brain. Plenum Press, NY.

Popov VI, Davies HA, Rogachevsky VV, Patrushev IV, Errington ML, Gabbott PLA, Bliss TVP, Stewart MG (2004) Remodelling of synaptic morphology but unchanged synaptic density during late phase long-term potentiation (LTP): a serial section electron micrograph study in the dentate gyrus in the anaesthetized rat. Neuroscience 128:251–262.

Popov V, Medvedev NI, Davies HA, Stewart MG (2005) Mitochondria form a filamentous reticular network in hippocampal dendrites but are present as discrete bodies in axons: a three-dimensional ultrastructural study. J Comp Neurol 492:50–65.

Popov VI, Medvedev NI, Kraev IV, Gabbott PL, Davies HA, Lynch M, Cowley TR, Berezin V, Bock E, Stewart MG (2008) A cell adhesion molecule mimetic, FGL peptide, induces alterations in synapse and dendritic spine structure in the dentate gyrus of aged rats: a three-dimensional ultrastructural study. Eur J Neurosci 27:301–314.

Popov VI, Stewart MG (2009) Complexity of contacts between synaptic boutons and dendritic spines in adult rat hippocampus: three-dimensional reconstructions from serial ultrathin sections in vivo. Synapse 63:369–377.

Racine RJ (1972) Modification of seizure activity by electrical stimulation. II. Motor seizure. Electroencephalogr Clin Neurophysiol 32:281–294.

Ratzliff ADH, Santhakumar V, Howard A, Soltez I (2002) Mossy cells in epilepsy: rigor mortis or vigor mortis? Trends Neurosci 25:140–144.

Ribak CE, Korn MJ, Shan Z, Obenaus A (2004) Dendritic growth cones and recurrent basal dendrites are typical features of newly generated dentate granule cells in the adult hippocampus. Brain Res 1000:195–199.

Ribak CE, Shapiro LA (2007) Ultrastructure and synaptic connectivity of cell types in the

adult rat dentate gyrus. Prog Brain Res 163:155–166.

Ribak CE, Shapiro LA (2007) Dendritic development of newly generated neurons in the adult brain. Brain Res Rev 55:390–394.

Scott BW, Wang S, Burnham WM, De Boni U, Wojtowicz JM (1998) Kindling-induced neurogenesis in the dentate gyrus of the rat. Neurosci Lett 248:73–76.

Segal M (2005) Dendritic spines and long-term plasticity. Nat Rev Neurosci 6:277–284.

Seri B, García-Verdugo JM, Collado-Morente L, McEwen BS, Alvarez-Buylla A (2004) Cell types, lineage, and architecture of the germinal zone in the adult dentate gyrus. J Comp Neurol 478:359–78.

Shapiro LA, Ribak CE and Jessberger S (2008) Structural changes for adult-born dentate granule cells after status epilepticus. Epilepsia 49 (Suppl 5):13–18.

Shapiro LA, Figueroa-Aragon S, Ribak CE (2007) Newly generated granule cells show rapid neuroplastic changes in the adult rat dentate gyrus during the first five days following pilocarpine-induced seizures. Eur J Neurosci 26:583–592.

Schuster T, Krug M, Wenzel J (1990) Spinules in axospinous synapses of the rat dentate gyrus: changes in density following long-term potentiation. Brain Res 523:171–174.

Smith PD, McLean KJ, Murphy MA, Turnley AA, Cook MJ (2005) Seizures, not hippocampal neuronal death, provoke neurogenesis in a mouse rapid electrical amygdale kindling model of seizures. Neuroscience 136:405–415.

Smith PD, McLean KJ, Murphy MA, Turnley AM, Cook MJ (2006) Functional dentate gyrus neurogenesis in a rapid kindling seizure model. Eur J Neurosci 24:3195–3203.

Sorra KE, Harris KM (1998) Stability in synapse number and size at 2 hr after long-term potentiation in hippocampal area CA1. J Neurosci 18:658–671.

Spacek J, Lieberman AR (1980) Relationships between mitochondrial outer membranes and agranular reticulum in nervous tissue: ultrastructural observations and a new interpretation. J Cell Sci 46:129–147.

Spacek J, Harris KM (2004) Trans-endocytosis via spinules in adult rat hippocampus. J Neurosci 24:4233–4241.

Stewart MG, Davies HA, Sandi C, Kraev IV, Rogachevsky VV, Peddie CJ, Rodriguez JJ,

Cordero MI, Donohue HS, Gabbott PL, Popov VI (2005) Stress suppresses and learning induces plasticity in CA3 of rat hippocampus: a three-dimensional ultrastructural study of thorny excrescences and their postsynaptic densities. Neuroscience 131:43–54.

Tang L, Hung CP, Schuman EM (1998) A role for the cadherin family of cell adhesion molecules in hippocampal long-term potentiation. Neuron 20:1165–1175.

Toni N, Laplagne DA, Zhao C, Lombardi G, Ribak CE, Gade FH, Schinder AF (2008) Neurons born in the adult dentate gyrus form functional synapses with target cells. Nature Neurosci 11:901–907.

Tuunanen J, Pitkänen A (2000) Do seizures cause neuronal damage in rat amygdala kindling? Epilepsy Res 39:171–176.

Umeoka S, Miyamoto O, Janjua NA, Nagao S, Itano T (2000) Appearance and alteration of TUNEL positive cells through epileptogenesis in amygdaloid kindled rat. Epilepsy Res 42:97–103.

Yan XX, Spigelman I, Tran PH, Ribak CE (2001) Atypical features of rat dentate granule cells: recurrent basal dendrites and apical axons. Anat Embryol 203:203–209.

Zhao C-S and Overstreet-Wadiche L (2008) Integration of adult generated neurons during epileptogenesis. Epilepsia 49 (Suppl 5):3–12.

Legends to Figures

Fig. 1. The pattern of EEG after discharges (ADs) and time courses of AD duration and severity of behaviour seizures during rapid hippocampal kindling. **(a)** 1, 2 and 3 on the plot are primary, secondary and tertiary components of AD, respectively, after 3 and 36 stimulations. **(b)** Time courses of a total AD duration (s) and severity of behavioural seizures (stages).

Figure 2. BrdU labelling of scar on 11 day after implantation of electrodes. **A, C,** organization of scar projection on two consecutive 50 ⌠m sections in right hippocampus at a low magnification, and **B, D,** same images at a large magnification, correspondingly for **A** and **C**. **E**, some details of dentate gyrus BrdU labelling boxed in Fig. D. These images show that at least during the first 10 days there is intense mitotic activity of cells within scar (Fig. A, C labelling with black dotted line) including angiogenesis (blue arrows show postmitotic endothelial cells), gliosis (black arrows show astrocytes), and the presence of postmitotic cells (red arrows) in dentate gyrus: subgranular zone (SBZ); supragranular layer (SPGL); molecular layer of dentate gyrus and hilus. Abbreviation: bv, blood vessels/capillaries; fis, fissure.

Figure 3. The number of BrdU-labelled cells per right and left dorsal portions of dentate gyrus in control (without electrical stimulation) and after kindling (3 animals per group) is shown. From each perfused brain serial coronal sections (50 ⌠m in thick) were obtained and 30 sections were taken for quantitative analysis. Dorsal portions of left and right hippocampi only were analysed. There is a significant increase in BrdU labelled cells for kindling only (P = 0.01).

Figure 4. DCX and GFAP immunolabelling of 50 ⌠m sections of hippocampi. **A, C,** dorsal portions of left hippocampi. **B, D,** dorsal portions of right hippocampi out of scar zone from

rats subjected to partial kindling. **E,** GFAP labelled astrocyte from hilus of left dorsal hippocampus from control animal. **F**, GFAP labelled astrocyte from hilus of right dorsal hippocampus from rat subjected to kindling.

Figure 5. Relative volume of astrocytes in DG using 50 ⌠m sections, where the volume of astrocytes in the hilus of left hippocampi was taken as 100% (for details see Methods). There is a significant difference between astrocytic volume in the right and left DG of control unstimulated rats, presumably due to the presence of the electrode in the right DG of the unstimulated control rats. Following kindling the percentage volume of astroglia in the unstimulated hemisphere increases to that of the stimulated hemisphere. Each group consisted of 3 animals which were injected with BrdU.

Figure 6. A-E, DCX labelling of immature granule cells in subgranular zone (SGZ) of DG after partial kindling in right hippocampus. (A) shows low power of hippocampus with a dark band of DCX labelled cells. (B) Medium power of DG and SGZ; straight arrows show apical dendrites. (C-E) micrographs at increasing power of DCX labelled cells, again straight arrows show apical dendrites whilst curved arrows show basal dendrites. Neuronal bodies are marked by stars. Other abbreviations: DG, dentate gyrus; H, hilus; scale bars = 50 ⌠m

Figure 7. Eight consecutive serial ultrathin images (A-H) of granule cell dendrite (Den) in right hippocampus after rapid kindling. Mitochondrion (Mt) locks the base of neck of dendritic spine (S); however, spine apparatus and cisterns of smooth endoplasmic reticulum are absent. Higher power micrographs (I and J) show very clearly the locking of the base of the spine by the mitochondrion. Generally, such an interaction between mitochondrion and the base of a dendritic spine is accompanied with the absence of spine apparatus. Partial kindling stimulates, within dendroplasm, the formation of filamentous material which is structurally very similar to PSDs. Other abbreviations: PSD, post synaptic density, PrB pre-

synaptic bouton. mt, microtubules, V, presynaptic vesicles.

Figure 8. Ultrathin images and three-dimensional reconstructions showing details of synaptic structures: dendritic spines; PSDs; spinules and mitochondria. A-E, five consecutive images show 'giant' spinule (Sp) originating from dendritic spine head. F-G, three-dimensional reconstruction shows dendritic spine with the spinule. H-K, three-dimensional reconstructions of dendritic segment, dendritic spines, spinules, multi-vesicular body, smooth ER (endoplasmic reticulum) and mitochondrion after kindling. Other abbreviation: PrB, presynaptic bouton.

Figure 9. Ultrastructural organization of mushroom and thin spines after kindling. A-D, mushroom (Msp1) and thin (Tsp) dendritic spines. Typical mushroom spines contain spine apparatus (sa), cisterns of smooth ER (sER), multi-vesicular bodies, spinule/spinules (solid arrows) on their heads in contrast to thin spines. Rough ER (rER) and polyribosomes (prb) were revealed in the base of many mushroom and thin dendritic spines. E-G, spine apparatus and multi-vesicular bodies were characteristic features of mushroom spines.
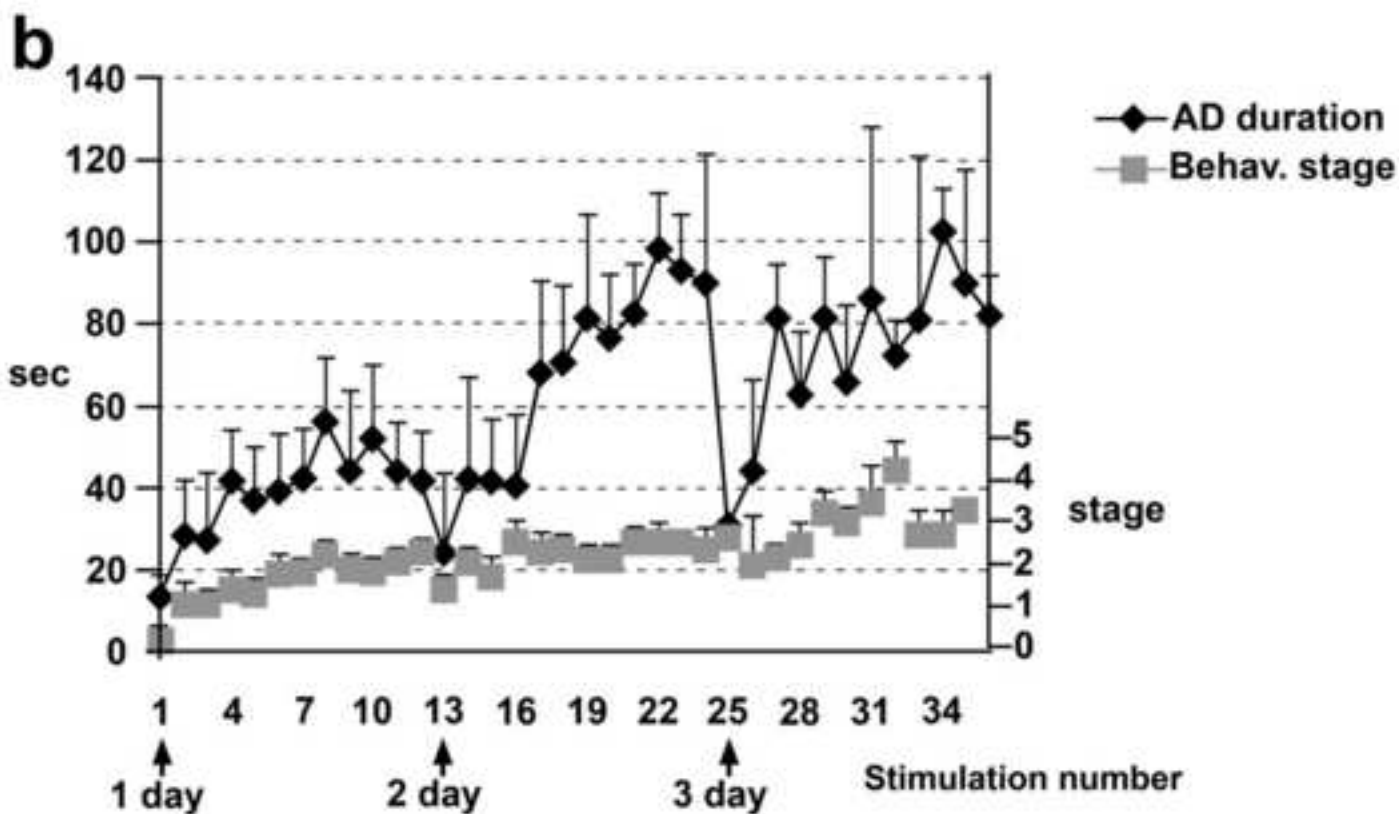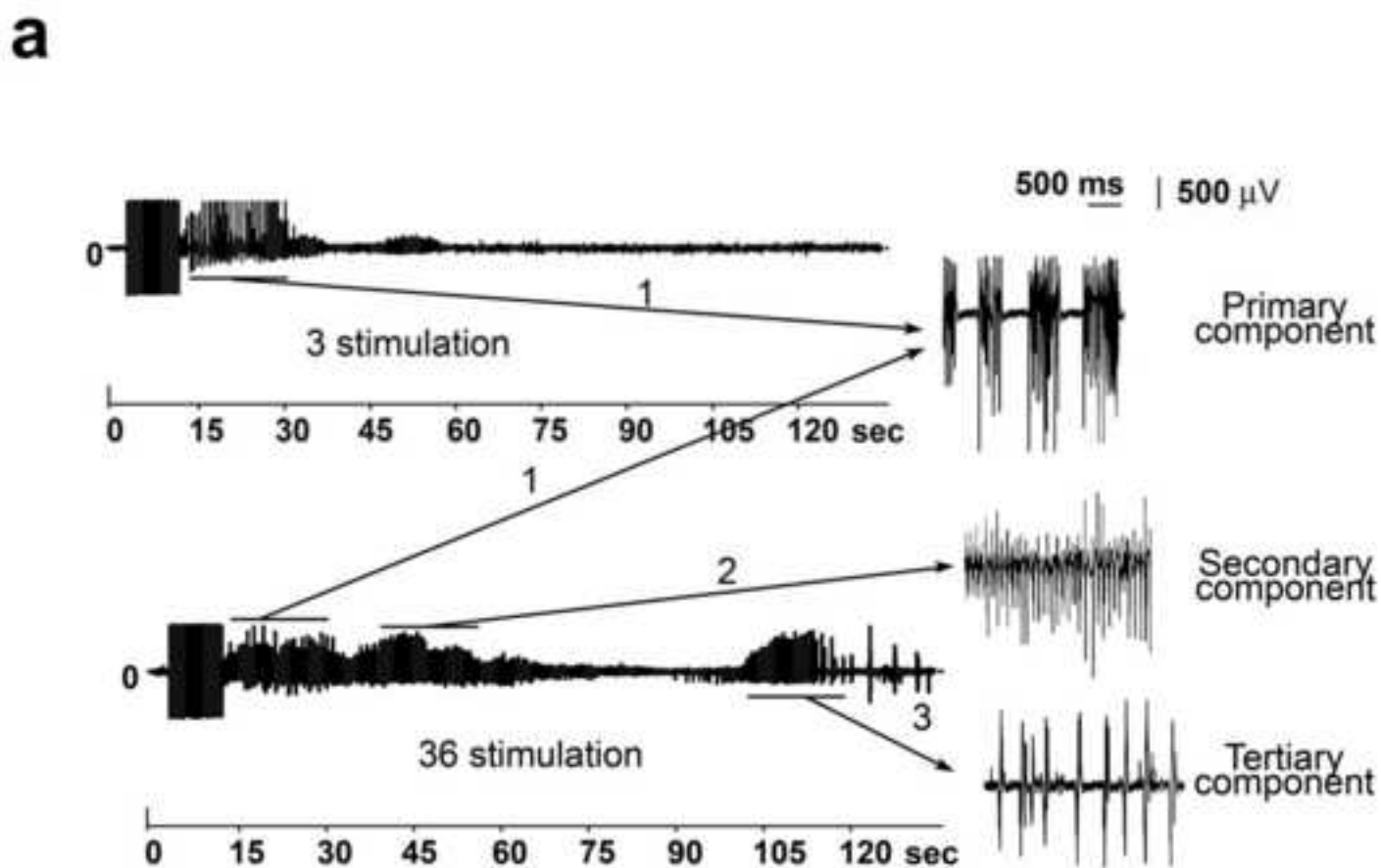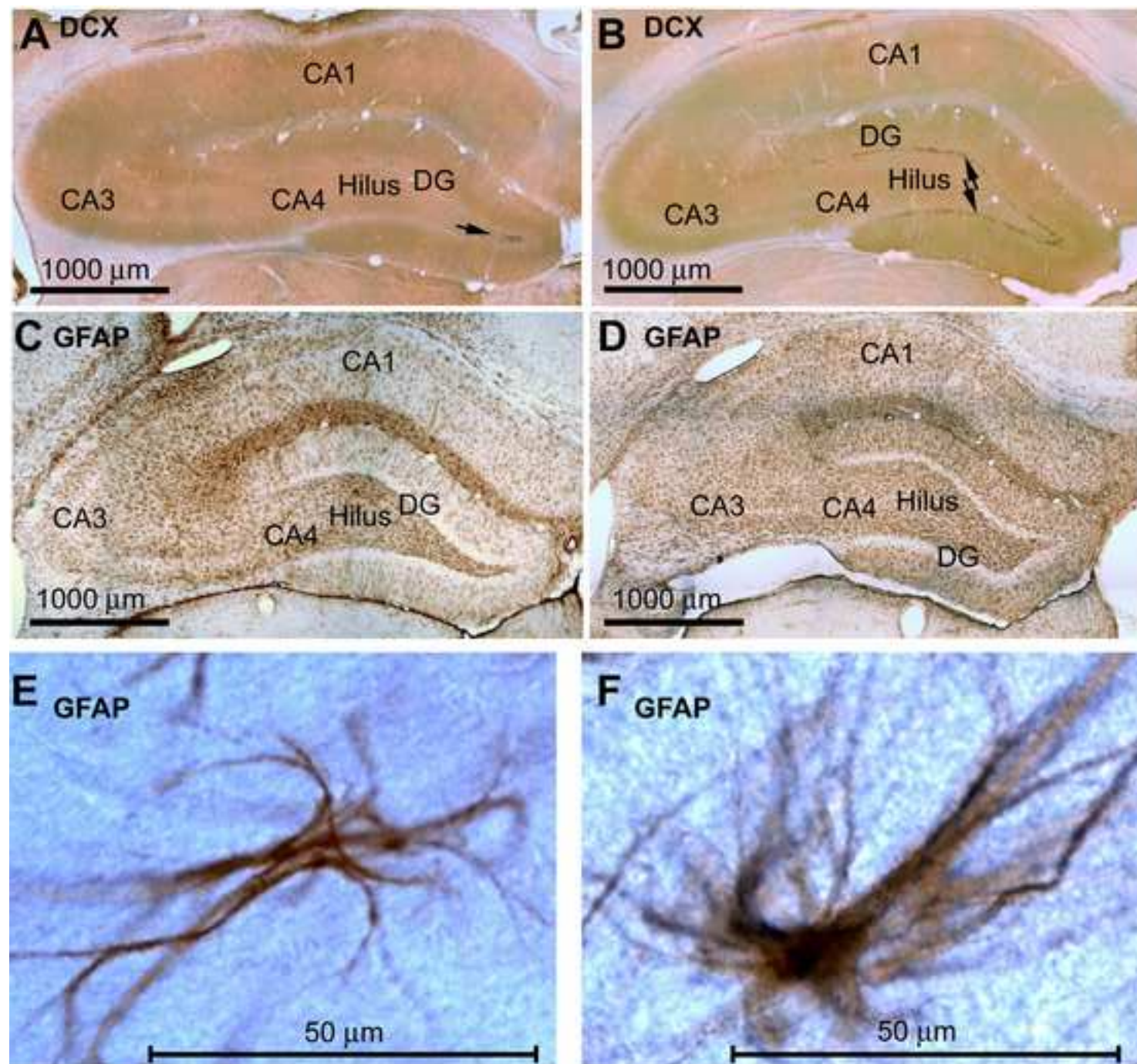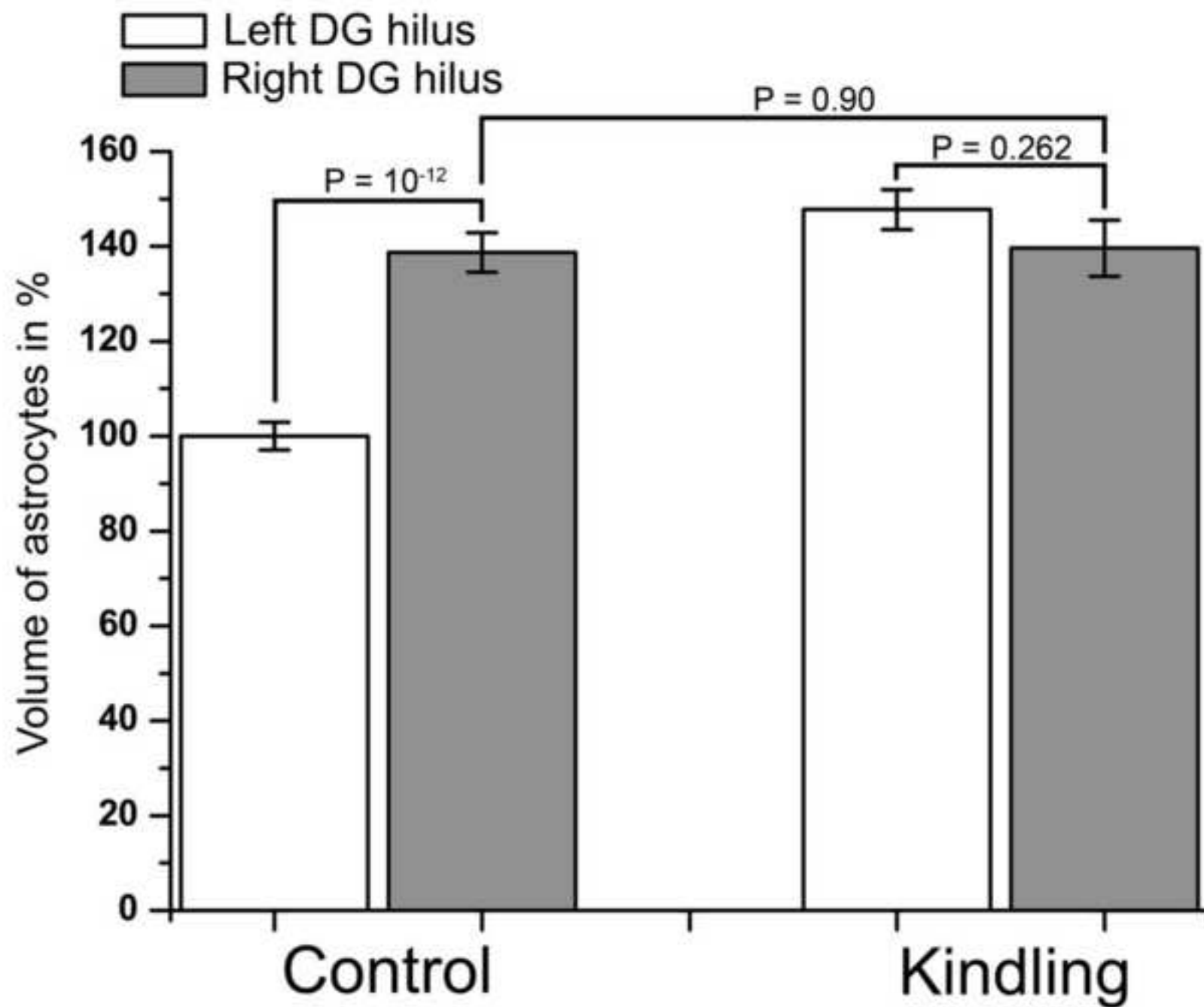
Figure 1
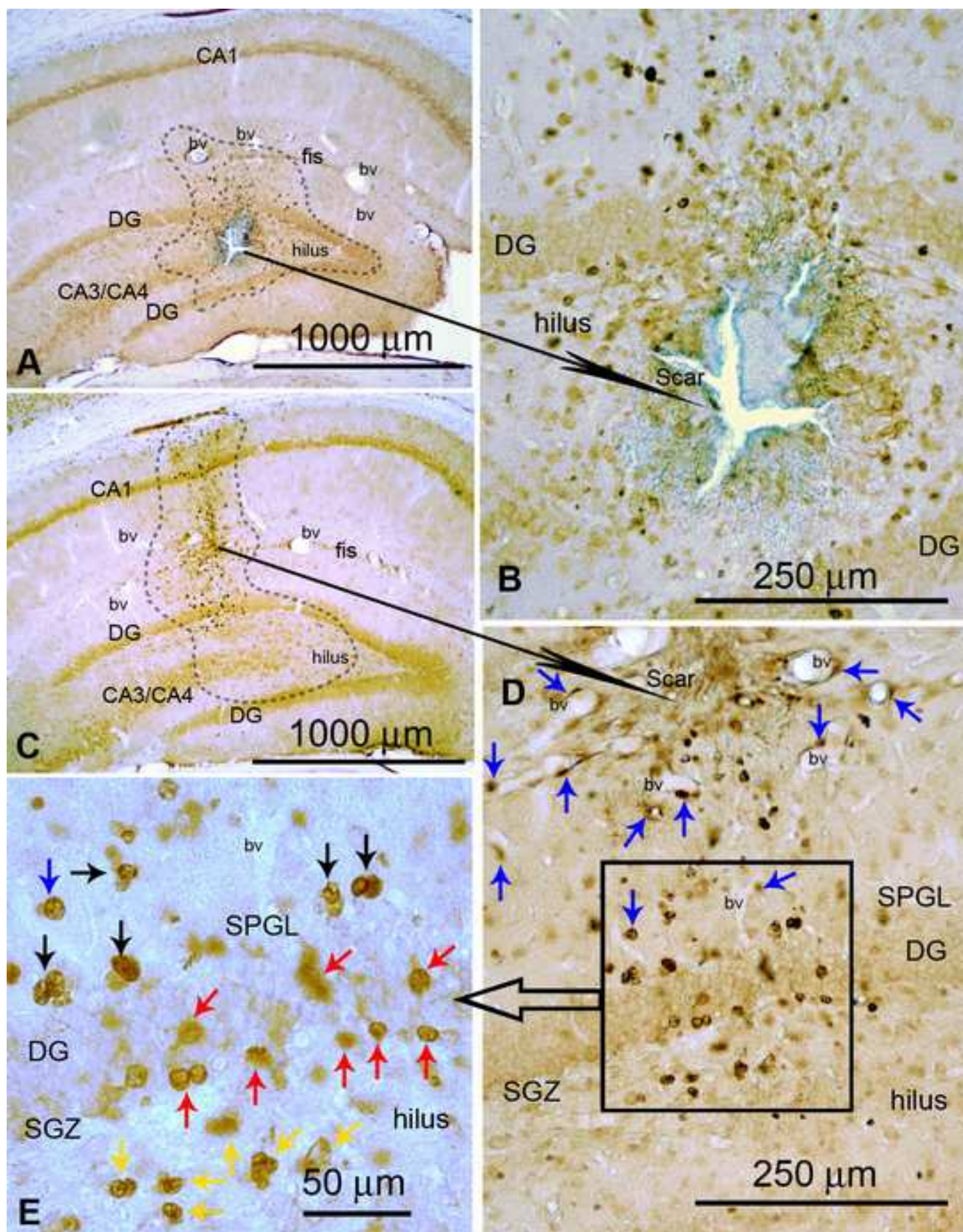
Figure 2
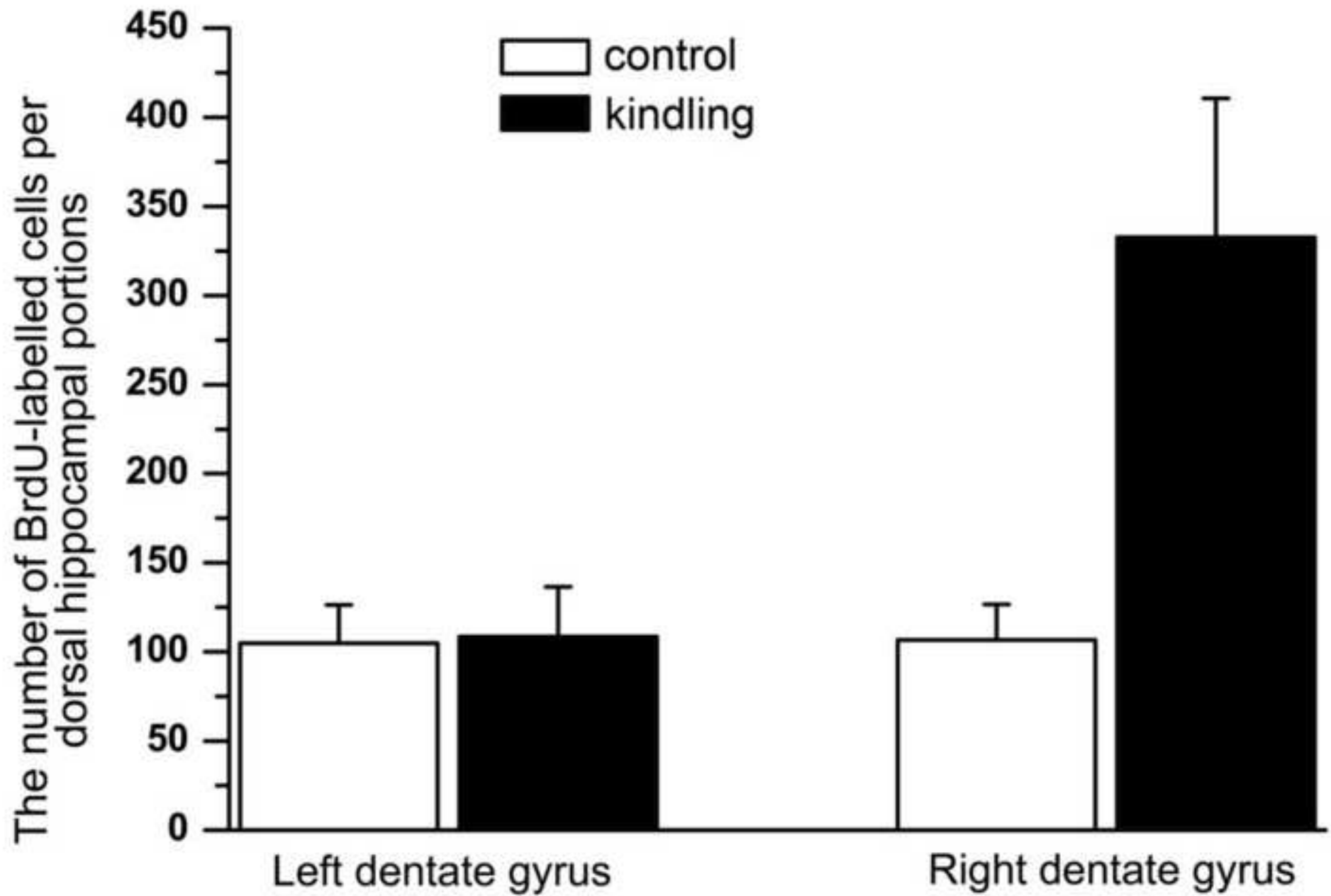
Figure3

Figure4

Figure
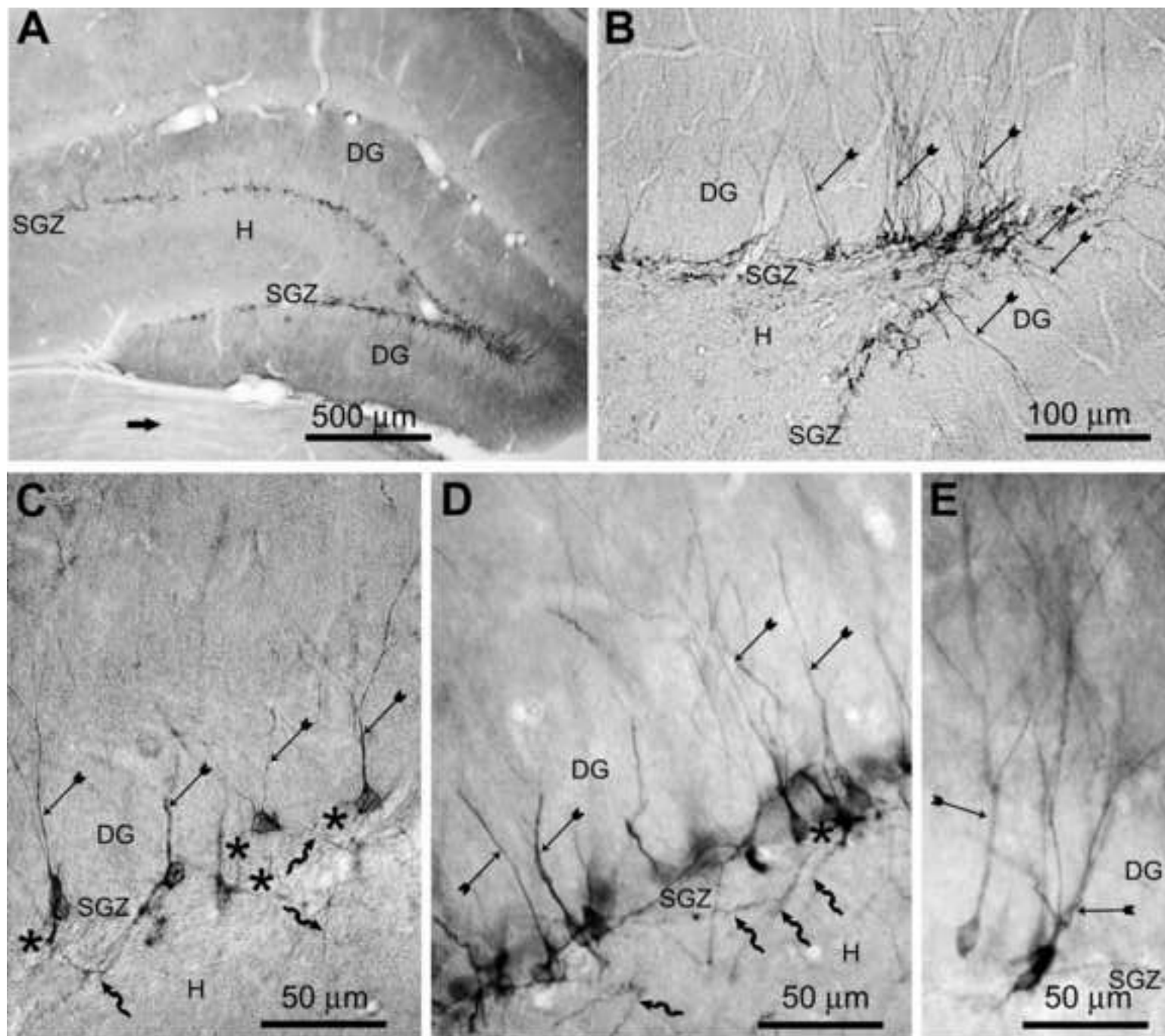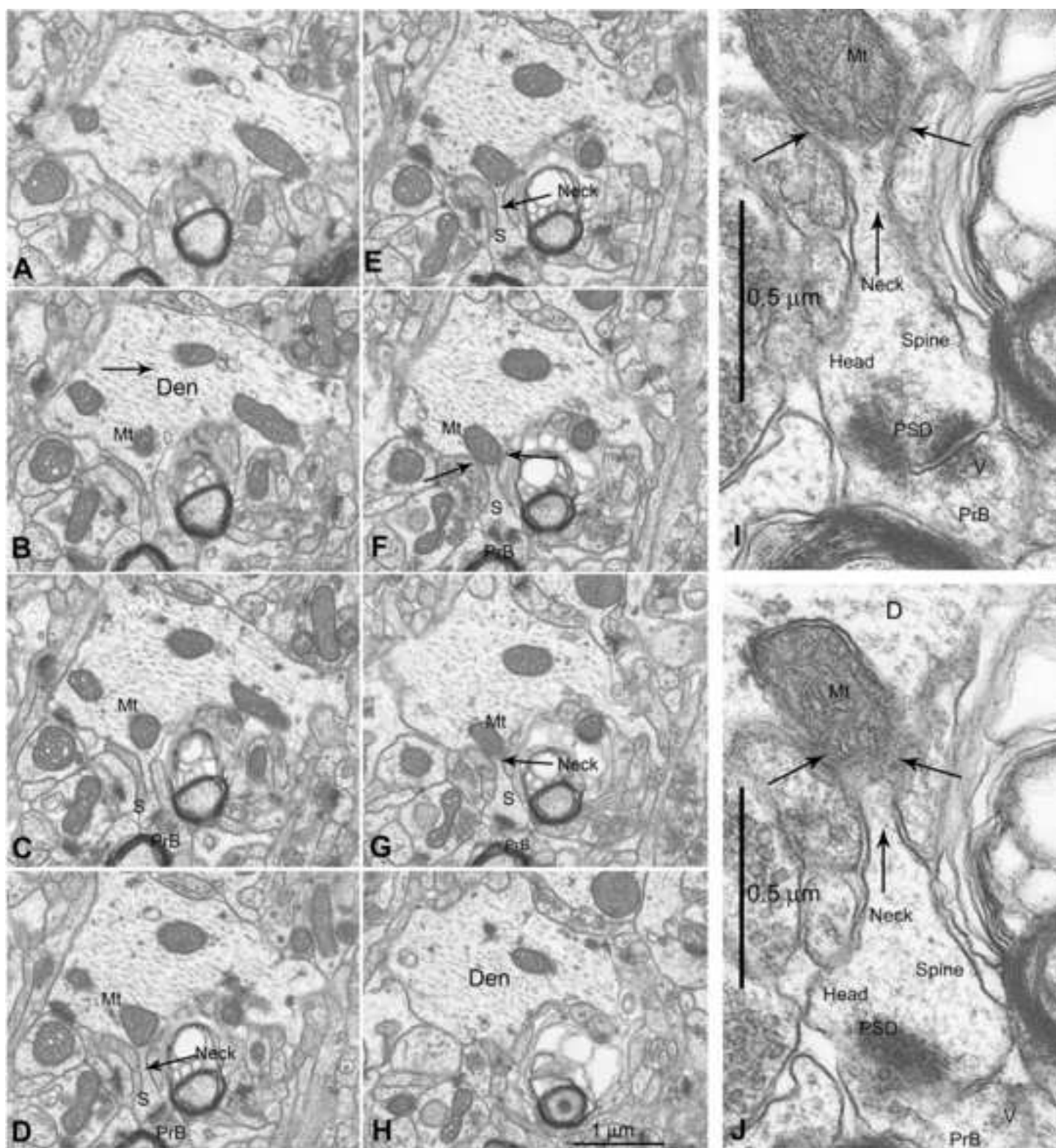
Figure5

Figure6

Figure7

Figure8

Figure9